Acta Crystallographica Section D
Biological Crystallography
ISSN 0907-4449

Reproducible growth of well diffracting ribosomal crystals

Tamar Auerbach-Nevo,* Raz Zarivach, Moshe Peretz and Ada Yonath

Department of Structural Biology, Weizmann Institute of Science, Israel

Correspondence e-mail: tamar.auerbach@weizmann.ac.il

Received 24 June 2004
Accepted 28 February 2005

The crystallization of ribosomal particles is associated with extraordinary challenging demands. This originates mainly from the ribosome's natural tendency to deteriorate and from its multi-conformational heterogeneity, both of which stem from its functional flexibility. To increase the level of homogeneity of ribosomal preparations, systematic searches for conditions yielding populations of fully defined chemical compositions were employed and the variables essential for high functional activity were analyzed and optimized. These include temperature, cell-growth duration and media, the cell-harvesting stage, ribosomal purification and storage. The functional state that is most suitable to yield quality crystals was identified as that of the polysome and it was found that this fraction reproducibly yielded crystals of superior properties.

1. Introduction

Ribosomes are ribonucleoprotein particles that exist in all living cells, be they of prokaryotic or eukaryotic origin, single cells, or in cell assemblies. Ribosomes play a key role in protein biosynthesis. In this process the information that is encoded in the nucleic acid sequence of the mRNA is translated into sequential polymerization of amino acids. These large assemblies have the ability to deal with two fundamentally different alphabets: the nucleic acids of the RNA and the amino acids of the proteins.

Ribosomes from all species display great structural and functional similarities. They are composed of two independent subunits of unequal sizes, which associate upon initiation of protein biosynthesis. The prokaryotic ribosome has a mass of about 2.45×10^6 Da; about two-thirds of the mass is constituted of RNA. Prokaryotic ribosomes are particles with a sedimentation coefficient of 70S. They are composed of a large, 50S subunit (1.45 MDa), and a small, 30S subunit (0.85 MDa). The 70S complex exists while the ribosome is translating.

The sequential assemblage of active simultaneously translating ribosomes that associate with one messenger RNA (mRNA) molecule are called polysomes. The parallel synthesis of several ribosomes on the mRNA increases the efficiency with which the mRNA is utilized. Within the polysomes each ribosome works independently at the polypeptide synthesis stage of translation. This arrangement is stable until all of the ribosomes reach the stop codon and dissociate from the mRNA or until the mRNA is degraded, under unfavorable circumstances. It can be expected that non-active ribosomes exist in the cell due to disintegration over time, decomposition of rRNA or partial deterioration. These are unlikely to take part in protein biosynthesis.

Protein biosynthesis is a multi-step cyclic process. The small subunit has key roles in initiation of translations, choosing the correct reading frame, decoding of the genetic message, discrimination against non- and near-cognate amino-acylated tRNA molecules and control of the fidelity of codon-anticodon interactions. The large subunit contains the peptidyl transferase center (PTC) and the protein exit tunnel. The PTC is the site of peptide bond synthesis, the process in which amino acids are added to the nascent polypeptide chain.

Ribosomes present a significant crystallization challenge, due to their enormous size, their natural tendency to deteriorate, their inherent functional heterogeneity and their internal flexibility. Our crystallographic studies on the ribosome began over two decades ago, when it was known that despite intensive worldwide attempts, *E. coli* ribosomes did not yield any suitable crystals. Assuming that the difficulties in the crystallization of *E. coli* ribosomes arose mainly from their rapid deterioration, we searched for bacterial sources expected to yield more stable ribosomes. At the initial stages of our studies, we used ribosomes from *Bacillus stearothermophilus,* a semi thermophile, to attempt crystallization (Yonath *et al.*, 1980). Although the crystals of *B. stearothermophilus* large ribosomal subunits were only marginally suitable for crystallographic analysis (Berkovitch-Yellin *et al.*, 1992; Weinstein *et al.*, 1989; Yonath *et al.*, 1984), this approach led to searches for alternative sources. We found that the key to obtaining crystals suitable for crystallographic studies was the use of ribosomes from extreme habitats (*e.g.* thermophilic, halophilic and radiation-resistant bacteria). These ribosomes proved to have a higher stability and formed crystals, which diffracted to reasonable resolution and thereby allowed data collection. Indeed, so far the only high- and medium-resolution crystallographic studies have been performed on small ribosomal subunit (T30S) and the whole ribosome (T70S) of the thermophile *Thermus thermophilus* (Schluenzen *et al.*, 2000; Wimberly *et al.*, 2000; Yusupov *et al.*, 2001), the large ribosomal subunit (H50S) of the halophilic archae *Haloarcula marismortui* (Ban *et al.*, 2000; Makowski *et al.*, 1987; von Bohlen *et al.*, 1991) and on the large ribosomal subunit (D50S) of the radiation-resistant eubacterium *Deinococcus radiodurans* (Harms *et al.*, 2001).

To obtain crystals that diffract to high resolution, homogeneous preparations are required. Several approaches were employed to overcome the low reproducibility of suitable preparations and the enormous functional variability, which leads to undesirable heterogeneity. Furthermore, we found that growing crystals under conditions approaching the *in situ* environments is a prerequisite for the determination of functionally relevant and fully ordered structures (Harms *et al.*, 2001; Yonath, 2002). Consistently, ribosomal crystals containing solutions that deviate significantly from the *in situ* environment, such as those of *H. marismortui* large subunit (H50S) yielded a high-resolution structure in which almost all functionally relevant components are disordered (Ban *et al.*, 2000).

It was previously shown that the addition of minute amounts of low-molecular-weight alcohols assists in the regaining functional activity of damaged ribosomal preparations (Vogel *et al.*, 1971; Zamir *et al.*, 1971) and maintaining or increasing the activity of functional ribosomes. We therefore adopted this procedure in our experiment. We found that in many cases pre-crystallization heating and the addition of minute amounts of low-molecular-weight alcohols led to crystal growth of ribosomal particles and that post-crystallization treatment could increase the resolution dramatically.

T30S crystals provide an example for post-crystallization rearrangements that led to marked improvement in resolution. The severe non-isomorphism of the original T30S crystals was minimized by the addition of a tungsten cluster, $[(NH_4)_6(P_2W_{18}O_{62})\cdot 14H_2O]$ (Dawson, 1953), hereinafter referred to as W18, which improved the resolution from <7 to 3.0 Å. This cluster played a dual role, as it also yielded phase information. Detailed analysis showed that all W18 clusters were attached to the ribosomal proteins, mainly at their elongated termini extensions (Fig. 1), in positions that may significantly reduce the global mobility of the T30S particles. Pairing of T30S particles around the crystallographic twofold axis is one of the main features of the map of T30S (Harms *et al.*, 1999). The contacts holding these butterfly-shaped pairs are extremely stable, such that they are maintained even after the rest of the crystal network is destroyed. Hence, large proportions of butterfly-shaped pairs have been observed by electron microscopy in samples of dissolved T30S crystals. Analysis of the mode of W18 binding showed that the pairing contacts reduced the mobility of protein S2, which in turn rigidified

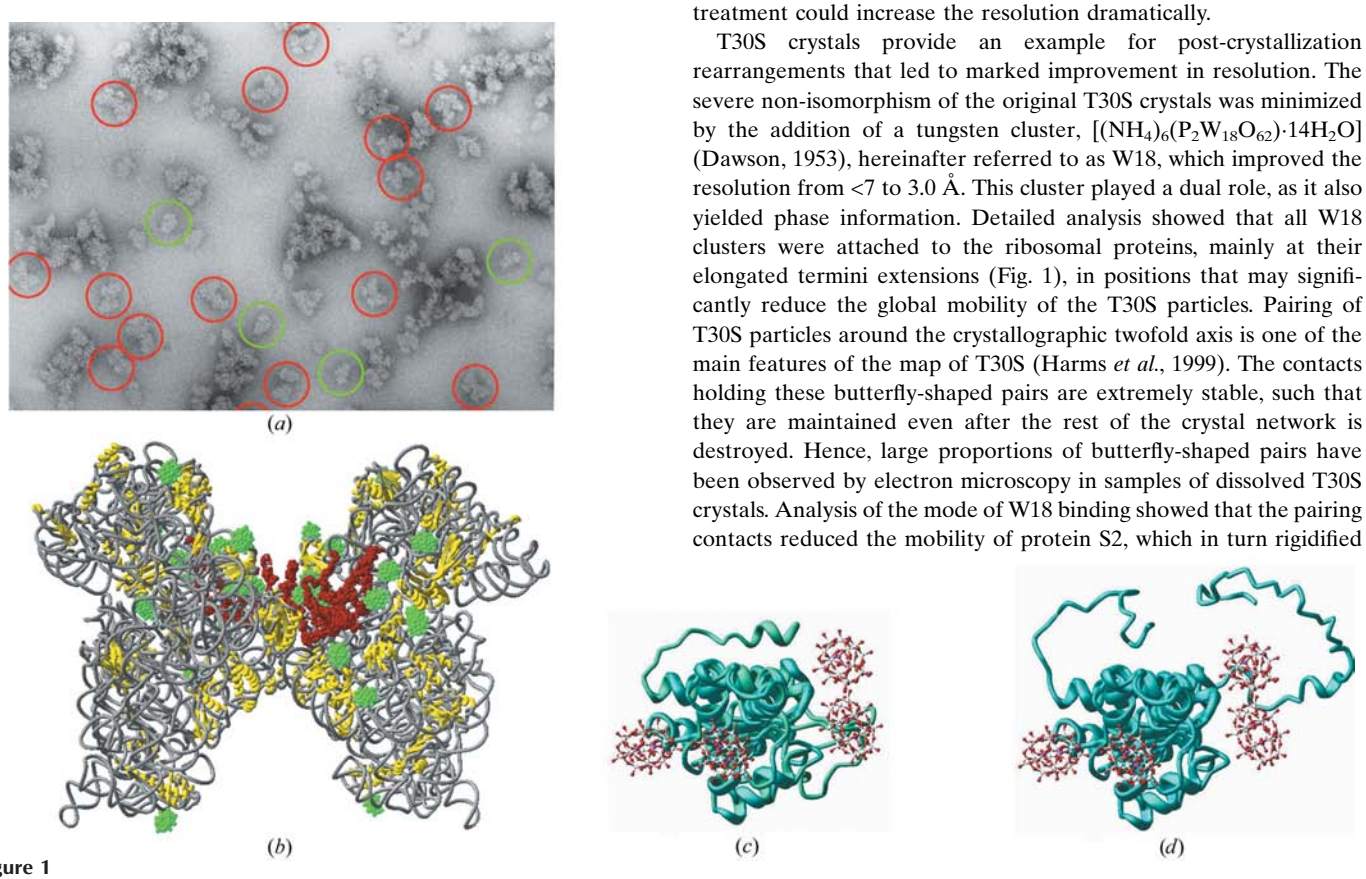

Figure 1
W18 binding to the T30S subunit. (*a*) Cryo-electron microscopy image of the dissolved T30S crystals. Isolated particles are encircled in green, pairs with butterfly shape are circled in red. An intensive net of contacts around the crystallographic twofold rotation axis, maintained even after the crystals were dissolved form these 'butterflies'. (*b*) Shows the two symmetry-related T30S particles in their crystallographic packing diagram, together with the W18 (in green); the ribosomal RNA backbone (in gray) and all the protein of small ribosomal subunit in yellow, except for protein S2 (in red), which creates most of the interactions between the two particles. This protein resides on the solvent side of the particle, combining the top (called the 'head') and the main part (called the 'body') of the particle. It is extremely flexible, as seen by comparing (*c*) and (*d*), which show the native and the W18-bound S2, respectively. The positions of four tightly bound W18 clusters, as seen in the W18-bound form, are shown on both images in order to indicate the reasons for the tremendous conformational alterations that both the N- and the C-termini of S2 undergo upon binding the closures. In the crystal, these termini intertwine around the twofold symmetry, creating an incredibly stable rather large contact area. Colour versions of the figures in this article are available in the online edition of the journal.

the flexible upper portion of the small subunit, accounting for almost a third of its mass (called the 'head'), namely about 250 Da, thus leading to a high-resolution structure (Schluenzen *et al.*, 2000; Tocilj *et al.*, 1999). In the T30S crystal this protein is positioned almost at the twofold rotation axis and is hence almost colliding with the same protein of the symmetry-related T30S subunit. The ability of both its termini to undergo amazing conformational changes upon the binding of four W18 clusters led to intersubunit interactions which allowed such positioning. Hence, this is one of the rare occasions of the preservation of crystallographic symmetry, even when most of the crystal network has been is lost.

Although the main factors for obtaining suitable crystals have been identified previously and the structures were elucidated, the determination of conditions for reproducible growth of quality crystals remains problematic. Here, we describe our successful attempts at improving crystal growth reproducibility and quality.

2. Materials and methods

2.1. Materials

Ingredients for the bacterial media were purchased from Oxoid and sucrose from Rhenium. All other chemicals were of analytical grade and obtained from Merck.

2.2. Strains

D. radiodurans cells isolated from irradiated ground pork and beef were obtained as a freeze-dried culture from ATCC (13939; Brooks & Murray, 1981). The genome was sequenced in 1999 by White and coworkers (White *et al.*, 1999). The cells were kept as glycerol stocks at 193 K.

2.3. Bacterial growth

Growth was started from a single colony at 303 K. Standard LB medium was used with an addition of 0.5% glucose. All chemicals for the medium were purchased from Oxoid. New Brunswick fermentors were used for experimental and batch growth. The bacteria were harvested at 277 K after reaching 2/3 log phase.

2.4. Ribosome purification

Ribosomes were purified using methods based on those described by Bloebel and coworkers (Erickson & Blobel, 1983). A few modifications were introduced in order to reach highly homogeneous and active preparations. Cells were disrupted using a French pressure cell press from American Instrument Company with a French pressure cell piston from Thermo Spectronic and Emulsiflex-C05 from Avestin. Zonal centrifugation was carried out with a Beckman Ti-15 rotor.

2.5. Polysome purification

The bacterial pellets were dissolved in 10 m*M* Tris pH 7.0, 7 m*M* $MgCl_2$, and 150 m*M* NH_4Cl. The cells were broken using a French press. DNase was added to a final volume of 0.1 µg ml^{-1} and incubated for 1 h at 283 K. Cell debris was removed by centrifugation at 30 000 rev min^{-1} for 90 min using a Type 70 rotor. The supernatant was centrifuged at 45 000 rev min^{-1} in a Type 70 rotor for 3 h. The resulting pellet consisted of polysomes alone. In order to dissociate the polysomes from the mRNA, extensive dialysis against 10 m*M* Tris pH 7.0, 0.5 m*M* $MgCl_2$ and 60 m*M* NH_4Cl was applied.

Table 1
Different growth media.

The core media which led the way to the improved growth media of *D. radiodurans*. In the first four columns the focal additives are listed with their concentration, in the last two columns, the maximal OD at 560 nm and the final pH of the culture are shown. Further experiments with the addition of $MnSO_4$ to different organic compounds did not generate any higher yield than OD_{560} = 14.45.

	Tryptone (g l^{-1})	Yeast (g l^{-1})	NaCl (g l^{-1})	Additive	Max OD	Final pH
1	10	5	5	—	3.36	7.43
2	10	5	5	0.5% glucose	3.54	6.37
3	20	10	15	—	3.54	7.23
4	10	5	5	3 g l^{-1} Na succinate	2.74	7.53
5	10	5	5	0.5% glucose, 1 g l^{-1} $MgSO_4$	4.92	6.96
6	10	5	5	0.5% glucose, 0.5 g l^{-1} KH_2PO_4	3.27	7.47
7	10	5	5	0.5% glucose, 1 mg l^{-1} $MnSO_4$	14.45	6.78

2.6. Poly-U Assay

Ribosomal activity was tested by Poly-U Assay (Nireberg & Matthaei, 1961), with minor modifications to the original procedure. The subunits were heat-activated when defrosted and minor amounts of ethanol were added to increase activity. The test was performed instantly at every purification step.

2.7. Crystallization

Crystals of polysomal ribosomes were obtained at 293 K by the hanging-drop vapor-diffusion technique. The droplets contained D50S ribosomal particles or their complexes in solutions containing the buffer optimized for efficient protein biosynthesis, namely 10 m*M* HEPES pH 7.8, 10 m*M* $MgCl_2$, 60 m*M* NH_4Cl and 6 m*M* β-mercaptoethanol.

Due to the variability in the chemical properties of the ribosomal preparations, exact conditions had to be determined for every preparation individually. Hence, various ratios of ethanol:2-ethylhexane-1,3-diol were used as the precipitant.

Crystals were immersed in freezing solution as described (Harms *et al.*, 2001), mounted on cryoloops (Hampton Research Corporation) of a matching size, instead of the previous home-made double spatula, and flash-frozen in liquid propane or liquid nitrogen. Data were collected with well focused monochromatic X-ray beam at third-generation synchrotrons.

3. Results and discussion

3.1. High-yield growth

Owing to the inherent variability of the ribosomal crystals, their fragility and their severe radiation sensitivity, large quantities are essential for efficient ribosome crystallography. Thus, to minimize the need for merging crystallographic data generated from several preparations, which is a problematic issue in ribosomal crystallography, each individual preparation should be of an amount sufficient for screening the suitable crystallization conditions (see §3.5), as well as for final crystallization, co-crystallization and soaking. Hence, to achieve the highest possible yield from each preparation, various cell-growth conditions were employed, aiming at obtaining maximum ribosomal activity within the log phase during cell growth. Since we found that best crystals are obtained from cells harvested during their log phase, efforts were made to extend the log-phase growth.

Optimization of the *D. radiodurans* growth was carried out in different media, by varying the pH, the additives and their sources. Since *D. radiodurans* is an organotroph eubacterium, the effect of the addition of different organic compounds to the medium was tested

(see Table 1). Glucose was found to be an important additive for obtaining ribosomes with a high activity, since the addition prevents long lag phases and starvation of the cells. Further trials with the addition of different salts and trace elements to the medium did not increase the yield, with the exception of $MnSO_4$.

The addition of Mn^{2+} at 2.5 μM or higher to stationary-phase cultures of *D. radiodurans* was found to trigger at least three rounds of cell division (Chou & Tan, 1990). Indeed, the addition of Mn^{2+} to the medium proved to extend the log phase of *D. radiodurans*. A tenfold extension of the log phase improved the yield by tenfold. The yield of a 10 l fermentor without addition of $MnSO_4$ correlates to about 14 g, compared to 105 g when $MnSO_4$ is included from the beginning.

Sodium citrate was found to increase the amount of active ribosomes (Widmann & Sussmuth, 1978). The sodium citrate was filtered separately and added to the medium before inoculation. As a result of the citrate addition, even fractions showing a lower activity rate than the high-activity ribosomes gave stable, albeit small, crystals.

Finally, the tryptone in the growth medium was found to be of enormous importance. Similar media, such as Difco, Merck and Oxoid, were tested and only the latter was found to yield batches with crystallizable ribosomes. Only cells grown on media prepared with tryptone from Oxoid exhibited the typical quadruple formation of *D. radiodurans* cocci. When grown on LB media from Difco the cells aggregated to clusters. The well organized looking cells and the crystals obtained from these batches left the conclusion that the growth of the cells is more steady and balanced than when using tryptone from other suppliers. A more detailed analysis of the tryptone showed that the concentration of manganese ions is higher in the Oxoid tryptone, which as discussed above is important for high-yield growth of *D. radiodurans*.

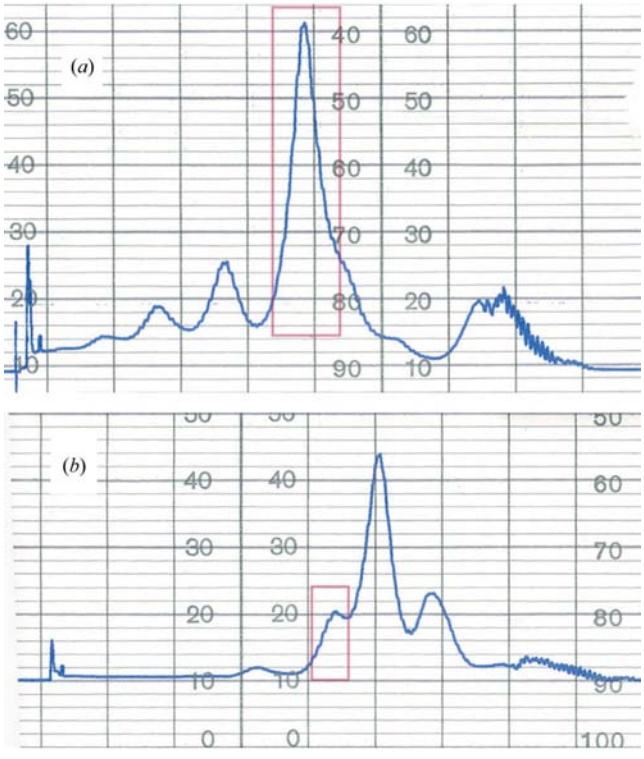

Figure 2
Polysomes (*a*) and their separated 50S and 30S subunits (*b*) on an analytical gradient. The pink rectangle highlights the 70S peak. In the analytical run of the dissolved polysome pellet the 70S peak is preceded by peaks that consist of particles with a higher sedimentation coefficient (≥70S). There are no peaks of separate 30S and 50S subunits. After dialysis the 70S and polysomal assemblies fall apart fully to yield 30S and 50S subunits.

Table 2
Pressure *versus* crystals.

Cell disruption with two different apparatuses: a continuous pressure cell press and a piston pressure cell and their dependence on yielding crystallizable material.

Pressure device	Pressure (p.s.i.) × rounds	Crystals obtained
French press	6000 × 2	Yes
French press	8000 × 2	Yes
French press	11000 × 1	Yes
French press	11000 × 2	Partly
French press	13000 × 1	No
French press	16000 × 1	No
French press	18000 × 1	No
Emulsiflex	14000 × 1	No
Emulsiflex	16000 × 1	No

3.2. Cell disruption

Several methods are commonly used to disrupt cells for ribosome extraction from bacteria, including enzymes, solvents, sonication, pressure and mechanical disruption. However, most of them were found not to be satisfactory for preparing *D. radiodurans* ribosomes. Thus, grinding is time-consuming; there are no enzymes that disrupt Gram-positive cells; solvents and antimetabolites that disrupt the cell membrane do not lyse the cells effectively; and sonication causes deterioration of the ribosomal RNA (rRNA). By contrast, pressure disruption is fast, effective and reproducible. Hence, superficially it is the method of choice, but practically even this step had to be carefully examined.

Pressure disruption was conducted with two different apparatuses: a continuous pressure cell press and a piston pressure cell. The continuous pressure cell was unable to disrupt *D. radiodurans* cells at 14 000 p.s.i. (1 p.s.i. = 6894.75 Pa) and preparations obtained by pressures beyond that did not yield any crystals, since the ribosomes were deteriorated. The piston-based pressure cell was unable to disrupt cells with a pressure less than 6000 p.s.i., while pressures beyond 11 000 p.s.i. did not yield crystallizable preparations. Hence, although the use of high pressure may result in a larger ribosomal

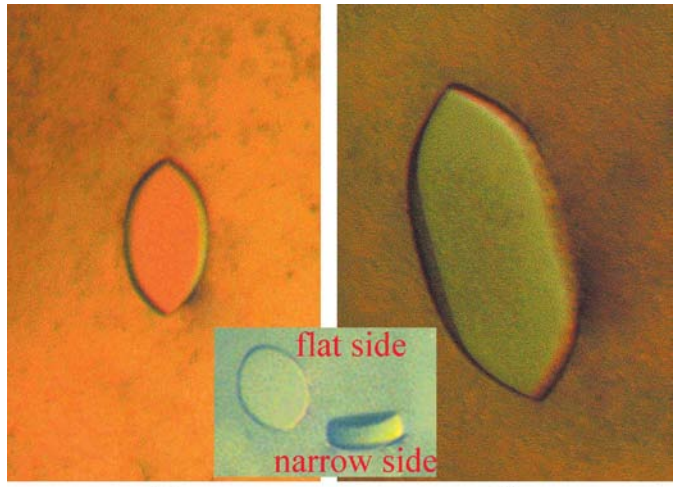

Figure 3
Appearance/shape of polysomal crystals. The crystals obtained from the polysome fraction are larger in size and thicker. The crystals are more elongated and the sides do not have sharp 90° angles between the flat and the narrow side, as the old preparations, but a smoother bending/connection between the two faces. The crystal in (*a*) is 170 µm in length, the crystal in (*b*) is 330 µm in length.

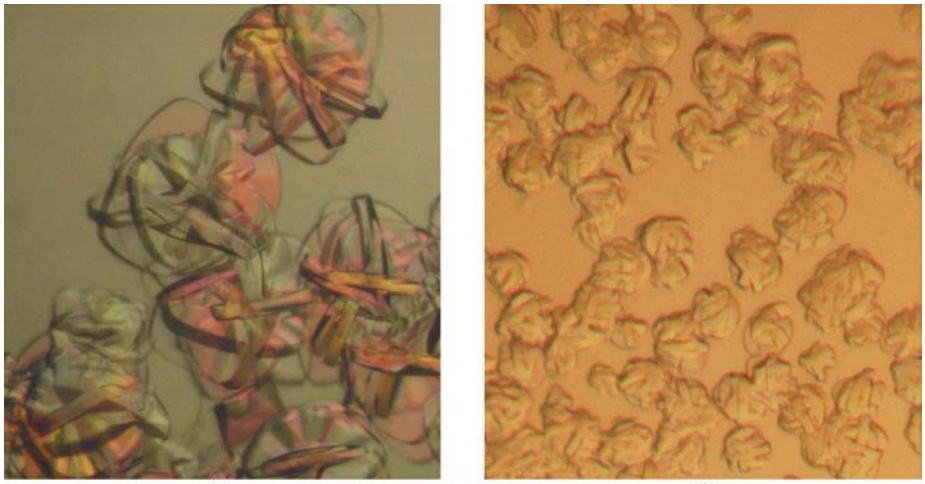

Figure 4
Cluster formation at high ribosomal concentrations (*a*) and the dependence of crystal formation on percentage of precipitant (*b*). The pictures were taken from drops crystallized with the same material as the crystal in Fig. 3(*b*). Crystals suitable for crystallographic work were only obtained after screening the concentration of the ribosome (as described in the text) and the precipitant in a range of ±3%. The same scale was used for (*a*) and (*b*) (750 µm from top to bottom).

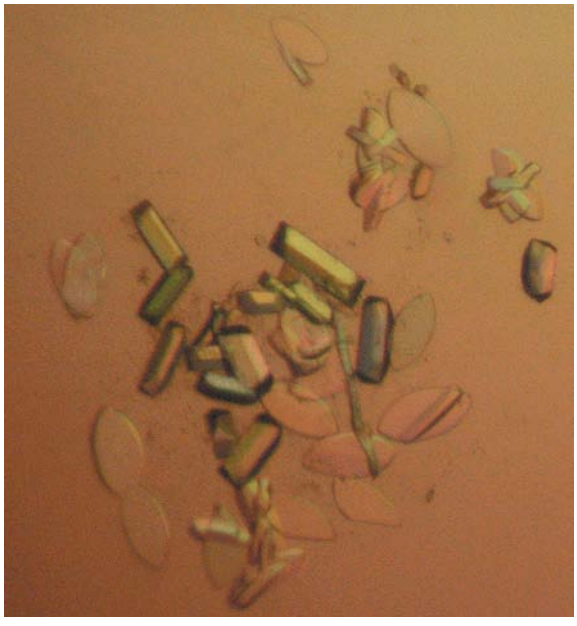

Figure 5
Salt-crystal formation within the ribosome preparation. Clearly visible are rectangular salt crystals, which are common using the former procedure (Schluenzen *et al.*, 2001). The largest crystals visible are 130 µm in length.

yield, it can also lead to RNA damage and, consequently, to non-crystallizable preparations, as shown in Table 2. Thus, only a narrow window was found to be suitable for active ribosome extraction. Furthermore, our experience shows that it is crucial to define the right pressure for each bacteria type, since different bacteria have different cell walls and different shapes.

3.3. Purification of polysomes

Applying the new purification procedure, both ribosomal subunits were successfully purified from the bacterial cells. As shown in Fig. 2, the crude polysome pellet consists of stable high-molecular-weight (≥70S) assemblies. Only after extensive dialysis the polysomal assemblies fell apart to its single constituents, the 30S and the 50S subunits. This purification ensured that all the 50S subunits are of the highest possible homogeneity and activity.

3.4. Activity of polysomes

We found a direct correlation between crystal quality and the activity and homogeneity of the ribosomes. The more active and homogeneous the material utilized, the faster crystallization occurs (two weeks *versus* 6–8 weeks) and the crystals obtained are of higher quality. To increase both ribosomal activity and homogeneity, the purification was modified so that a selected ribosomal fraction of the highest possible activity is being used for crystallization. As all ribosomes in the polysome fraction are occupied in protein biosynthesis, we purified ribosomal subunits from this fraction. The procedure for polysome purification yielded highly pure ribosomes, which were shown to be exceedingly active when tested by the common Poly-U assay. We also established that the faster the purification and the less freezing steps are employed during the procedure, improved ribosomal activity was achieved.

To further maintain the ribosomal homogeneity and activity, the ribosomes are heat-activated before being placed for the reaction and minute amounts of alcohol are added, as it was shown that both these steps increase ribosomal activity (Vogel *et al.*, 1971; Zamir *et al.*, 1971).

3.5. Crystallization and crystallographic analysis

The increased activity and homogeneity achieved through the use of polysomal ribosomes purification resulted in the formation of crystals within two weeks, as opposed to at least two months that were needed before the introduction of polysomal ribosomes. Furthermore, the polysomal crystals are bigger in size, thicker and have a different shape (Fig. 3) compared with the previous ones (Harms *et al.*, 2001). Hence, they provide a solution to one of the severe shortcomings of ribosomal crystallography, namely the thinness of the ribosomal crystals. In extreme cases, as for the original crystals of the large subunits from *H. marismortui* (Makowski *et al.*, 1987; Yonath *et al.*, 1988), the average crystal thickness was 1–3 µm. Obviously, these thin crystals are extremely fragile, readily bendable and behaved as built of sliding multi-layers.

As mentioned above, each ribosomal preparation has to undergo fine screening for its crystallization conditions. Although the same ingredients are used, minor changes in the amount of the precipitants or the ribosome concentration can cause an enormous change in crystal quality. One example is the appearance of clusters of thin and deformed crystals at a ribosomal concentration of 10.5 nmol ml^{-1}, compared with the large single crystals that are formed at 9 nmol ml^{-1} ribosomes (Fig. 4). Furthermore, minute variations in the precipitant can affect crystal shape and size (Fig. 4).

An additional problem encountered in D50S crystallization is the formation of salt crystals within the crystallizing droplets. In the previous crystal-growth procedure, when the crystallization process required a very long time (up to two months) we encountered a tendency for formation of salt crystals prior to ribosome crystal-

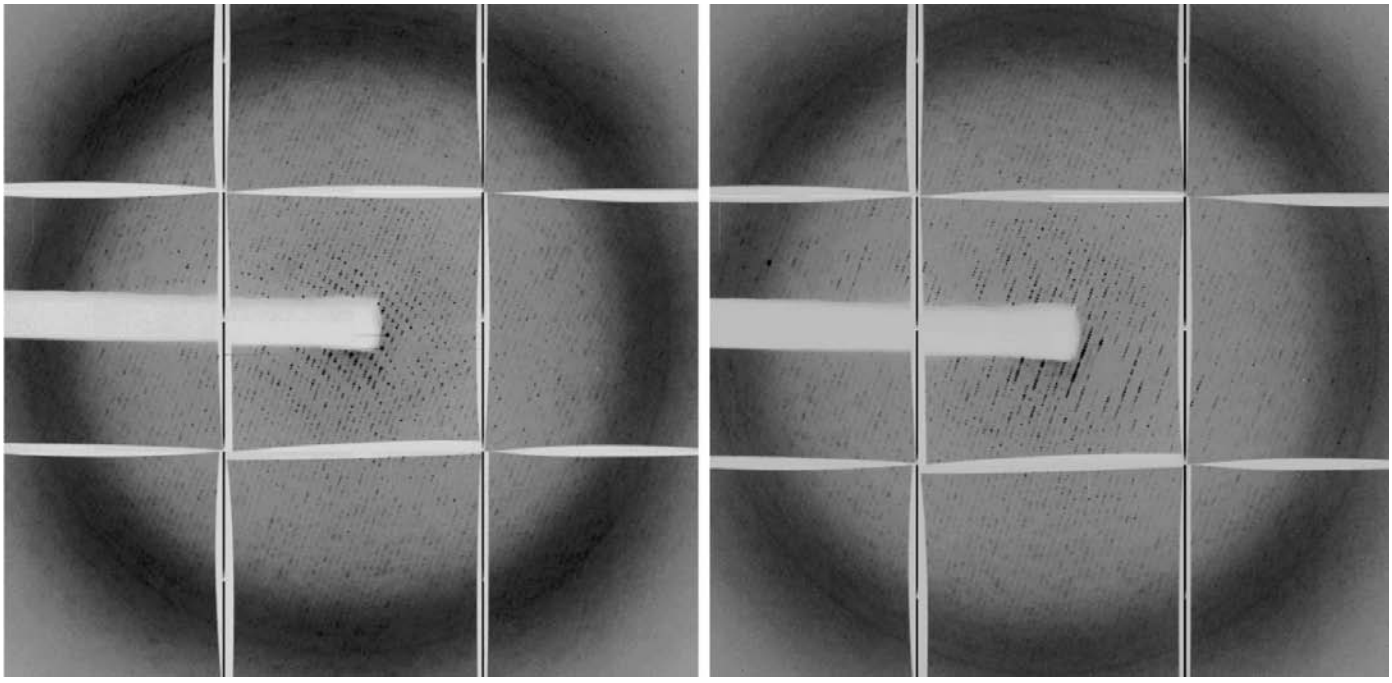

Figure 6
Two typical 0.1° rotation X-ray diffraction patterns obtained at 95 K with well collimated X-ray beams, at the high-brightness synchrotron-radiation station ID19/APS/ANL and recorded on the APS2 3×3 detector. The wavelength was 1.0332 Å, the collimator slits were 0.050 × 0.050 mm, the attenuation 0.5 and the crystal-to-detector distance was 300 mm. Note well resolved diffraction beyond the water ring.

lization. The appearance of salt crystals was sufficiently frequent to be used as an indication of the quality of the ribosomal preparation. Thus, the more salt crystals formed, the lower the chances for ribosome crystal formation (Fig. 5), perhaps because of increased ribosomal deterioration to fragments nucleating salt crystals.

The main advantages of the polysomal crystal type are the gain in the amount and quality of the crystallographic data that they generate. Thus, not only does their resolution extend to around 2.8 Å, but also typical single crystals yield around 65% of a complete data set compared to 25–40% of ∼3 Å data collected on average from previous crystals (Fig. 6). Collecting such a high number of data from single crystals should in turn yield higher quality merged data sets, since ribosomal crystals are still rather heterogeneous. These favorable properties, together with the improved crystal stability and more uniform shape, allow data collection in the commonly used loops instead of the homemade spatula designed for the thin and fragile crystals, which result in a lower background level.

Furthermore, similar to the mechanism, which led to the post-crystallization improvement in crystal order of T30S (described in §1), namely minimizing of riome flexibility, the D50S data quality was increased by co-crystallization with specific antibiotics. Examples are clindamycin (Schluenzen *et al.*, 2001) and a new compound, called AB-69 (Sittner *et al.*, work to be published). Both were found to reduce the flexibility of functionally relevant regions of the large ribosomal subunit. Thus, clindamycin is located between the PTC and the tunnel entrance (Schluenzen *et al.*, 2001) and AB-69 may have minimized the conformational flexibility of the L7/L12 stalk, which serves as the entry point of the A-site tRNA.

4. Conclusions

We showed that it is possible to produce large amounts of homogeneous highly active ribosomal particles by employing several approaches simultaneously. The addition of Mn^{2+} ions enabled us to obtain a tenfold yield of cells and the purification of polysomes ensured the use of ribosomal particles at a selected functional state for crystallization. Our systematic search for bacterial growth conditions, ribosome purification and crystallization procedures resulted in a gain in resolution and a fourfold faster crystallization, compared with our previous studies. Owing to the speedy purification and the shorter time the ribosomes spend in the crystallization drop, these macromolecular assemblies undergo a lower level of deterioration and disintegration, thereby yielding crystals of higher quality with enhanced resolution. Furthermore, as the polysome fraction always includes all of the active ribosomes within the cell, the procedure reported here is extremely reproducible.

Thanks are due to Heike Bartels, Anja Wolff, Christa Liebe, Miriam Laschever, Inbal Greenberg, David Baram, Anat Bashan, Assa Sittner, Haim Rozenberg, Erez Pyetan, Maggie Kessler, Maya Amit, Shlomit Maizel, Aharon Eliyahu and Amit Maor of the Weizmann Institute of Science for active involvement in the actual experiments, and to Andrew P. Seddon, Bruce Maguire and Senguil Han from Pfizer Global Reseach and Development, Groton, CT, USA for fruitful discussions. The crystallographic analysis was performed at BW6/MPG/DESY, ID14-4/ESRF/EMBL/Grenoble and ID19/SBC/APS/ANL beamlines. Support was provided by the US National Institutes of Health (GM34360), the Human Frontier Science Program Organization (HFSP: RGP0076/2003) and the Kimmelman Center for Macromolecular Assemblies. AY holds the Martin and Helen Kimmel Professorial Chair.

References

Ban, N., Nissen, P., Hansen, J., Moore, P. B. & Steitz, T. A. (2000). *Science*, **289**, 905–920.

Berkovitch-Yellin, Z., Bennett, W. S. & Yonath, A. (1992). *Crit. Rev. Biochem. Mol. Biol.* **27**, 403–444.

Bohlen, K. von, Makowski, I., Hansen, H. A., Bartels, H., Berkovitch-Yellin, Z., Zaytzev-Bashan, A., Meyer, S., Paulke, C., Franceschi, F. & Yonath, A. (1991). *J. Mol. Biol.* **222**, 11–15.
Brooks, B. W. & Murray, R. G. (1981). *Int. J. Syst. Bacteriol.* **31**, 353–360.
Chou, F. I. & Tan, S. T. (1990). *J. Bacteriol.* **172**, 2029–2035.
Dawson, B. (1953). *Acta Cryst.* **6**, 113–126.
Erickson, A. H. & Blobel, G. (1983). *Methods Enzymol.* **96**, 38–50.
Harms, J., Schluenzen, F., Zarivach, R., Bashan, A., Gat, S., Agmon, I., Bartels, H., Franceschi, F. & Yonath, A. (2001). *Cell*, **107**, 679–688.
Harms, J., Tocilj, A., Levin, I., Agmon, I., Stark, H., Kolln, I., van Heel, M., Cuff, M., Schlunzen, F., Bashan, A., Franceschi, F. & Yonath, A. (1999). *Structure Fold. Des.* **7**, 931–941.
Makowski, I., Frolow, F., Saper, M. A., Shoham, M., Wittmann, H. G. & Yonath, A. (1987). *J. Mol. Biol.* **193**, 819–822.
Nireberg, M. W. & Matthaei, J. H. (1961). *Proc. Natl Acad. Sci. USA*, **47**, 1588–1602.
Schluenzen, F., Tocilj, A., Zarivach, R., Harms, J., Gluehmann, M., Janell, D., Bashan, A., Bartels, H., Agmon, I., Franceschi, F. & Yonath, A. (2000). *Cell*, **102**, 615–623.
Schluenzen, F., Zarivach, R., Harms, J., Bashan, A., Tocilj, A., Albrecht, R., Yonath, A. & Franceschi, F. (2001). *Nature (London)*, **413**, 814–821.
Tocilj, A., Schlunzen, F., Janell, D., Gluhmann, M., Hansen, H. A., Harms, J., Bashan, A., Bartels, H., Agmon, I., Franceschi, F. & Yonath, A. (1999). *Proc. Natl Acad. Sci. USA*, **96**, 14252–14257.
Vogel, Z., Vogel, T., Zamir, A. & Elson, D. (1971). *J. Mol. Biol.* **60**, 339–346.
Weinstein, S., Jahn, W., Hansen, H., Wittmann, H. G. & Yonath, A. (1989). *J. Biol. Chem.* **264**, 19138–19142.
White, O. *et al.* (1999). *Science*, **286**, 1571–1577.
Widmann, A. & Sussmuth, R. (1978). *Z. Naturforsch. C*, **33**, 948–954.
Wimberly, B. T., Brodersen, D. E., Clemons, W. M. Jr, Morgan-Warren, R. J., Carter, A. P., Vonrhein, C., Hartsch, T. & Ramakrishnan, V. (2000). *Nature (London)*, **407**, 327–339.
Yonath, A. (2002). *Annu. Rev. Biophys. Biomol. Struct.* **31**, 257–273.
Yonath, A., Bartunik, H. D., Bartels, K. S. & Wittmann, H. G. (1984). *J. Mol. Biol.* **177**, 201–206.
Yonath, A., Glotz, C., Gewitz, H. S., Bartels, K. S., von Bohlen, K., Makowski, I. & Wittmann, H. G. (1988). *J. Mol. Biol.* **203**, 831–834.
Yonath, A., Muessig, J., Tesche, B., Lorenz, S., Erdmann, V. A. & Wittmann, H. G. (1980). *Biochem. Int.* **1**, 315–428.
Yusupov, M. M., Yusupova, G. Z., Baucom, A., Lieberman, K., Earnest, T. N., Cate, J. H. & Noller, H. F. (2001). *Science*, **292**, 883–896.
Zamir, A., Miskin, R. & Elson, D. (1971). *J. Mol. Biol.* **60**, 347–364.